ARTICLE

doi:10.1038/nature13470

Convergence of terrestrial plant production across global climate gradients

Sean T. Michaletz[1], Dongliang Cheng[2], Andrew J. Kerkhoff[3] & Brian J. Enquist[1,4,5,6]

Variation in terrestrial net primary production (NPP) with climate is thought to originate from a direct influence of temperature and precipitation on plant metabolism. However, variation in NPP may also result from an indirect influence of climate by means of plant age, stand biomass, growing season length and local adaptation. To identify the relative importance of direct and indirect climate effects, we extend metabolic scaling theory to link hypothesized climate influences with NPP, and assess hypothesized relationships using a global compilation of ecosystem woody plant biomass and production data. Notably, age and biomass explained most of the variation in production whereas temperature and precipitation explained almost none, suggesting that climate indirectly (not directly) influences production. Furthermore, our theory shows that variation in NPP is characterized by a common scaling relationship, suggesting that global change models can incorporate the mechanisms governing this relationship to improve predictions of future ecosystem function.

Annual net primary production (NPP; $\mathrm{g\,m^{-2}\,yr^{-1}}$) of woody plants is a major component of the terrestrial carbon cycle[1]. Although it has long been known that NPP correlates with mean annual temperature[2,3] and mean annual precipitation[3–5], efforts to understand the interactions between climate and metabolism have resulted in two conflicting generalizations. On the one hand, across a wide range of ecologically relevant temperatures, rates of photosynthesis and respiration increase approximately exponentially with temperature to a critical value beyond which rates decrease[6]. Furthermore, photosynthetic rate is limited by water availability, as reflected by a positive relationship between NPP and precipitation[4,5]. These patterns suggest that climate influences NPP directly via metabolic kinetics. On the other hand, across broad environmental gradients, local adaptation of thermal and edaphic tolerances may dampen physiological responses[7,8]. Under this scenario, correlations between NPP and annual climate variables result not directly from variation in metabolic rates, but rather indirectly via variation in plant size and stand biomass[8–10], stand age structure[7] and growing season length[10].

Metabolic scaling theory for NPP

To assess these differing viewpoints, we build upon metabolic scaling theory of forest structure and dynamics[11,12] to test the relative importance of direct and indirect climate effects on NPP (Supplementary Information). First, according to metabolic scaling theory, variation in instantaneous rates of respiration, photosynthesis and growth scale predictably with plant size and temperature. Second, extensions of metabolic scaling theory to whole-ecosystem functioning predict that NPP will scale with stand biomass and size of the largest individual[7,11–13]. Third, to incorporate the effects of temperature, precipitation, growing season length and plant age, we assume that their effects are inherently multiplicative[14]. As a result, hypothesized drivers of NPP can be assessed via the general equation

$$\mathrm{NPP} = P^{\alpha_P} l_{gs}^{\alpha_{l_{gs}}} a^{\alpha_a} e^{-E/kT} g_1 \frac{c_n}{A}\left[\frac{5{c_m}^{8/3}}{3c_n}\right]^{\alpha} M_{\mathrm{tot}}^{\alpha} \quad (1)$$

Here, the dependencies of NPP on precipitation P (mm), growing season length l_{gs} (months (mo) $\mathrm{yr^{-1}}$) and plant age a (yr) are characterized as power laws with exponents α_P, $\alpha_{l_{gs}}$ and α_a, respectively (Extended Data Fig. 1). This derivation permits evaluation of nonlinear relationships as well as a hypothesized direct proportionality between NPP and l_{gs} (that is, $\alpha_{l_{gs}} = 1$)[7,8]. The influence of temperature T (K) is characterized by an Arrhenius relation with an activation energy E (eV) and Boltzmann's constant k (8.617×10^{-5} $\mathrm{eV\,K^{-1}}$). An activation energy of 0.32 eV has been hypothesized for the kinetics of photosynthesis[15]. The influences of plant size and stand biomass are described by a size-corrected measure of the stand size distribution c_n (where $f(r) = \mathrm{d}n/\mathrm{d}r = c_n\, r^{-\alpha}$ and r is stem radius; m), a normalization constant c_m relating stem radius to plant mass ($r = c_m\, m^{3/8}$; $\mathrm{m\,g^{-3/8}}$), the total stand biomass M_{tot} (g), the stand area A ($\mathrm{m^2}$), and a growth normalization constant g_1 ($\mathrm{g\,m^{-1-\alpha(5/3)}\,yr^{-1+\alpha_{l_{gs}}-\alpha_a}\,mm^{-\alpha_P}\,mo^{-\alpha_{l_{gs}}}}$).

To best test metabolic scaling theory predictions and to evaluate direct and indirect climate effects, we recast equation (1) to give a more instantaneous monthly net primary production (NPP/l_{gs}; $\mathrm{g\,m^{-2}\,mo^{-1}}$) as

$$\frac{\mathrm{NPP}}{l_{gs}} = P^{\alpha_P} a^{\alpha_a} e^{-E/kT} g_2 \frac{c_n}{A}\left[\frac{5{c_m}^{8/3}}{3c_n}\right]^{\alpha} M_{\mathrm{tot}}^{\alpha} \quad (2)$$

where l_{gs} ($\mathrm{mo\,yr^{-1}}$) is growing season length and g_2 is another growth normalization constant ($\mathrm{g\,m^{-1-\alpha(5/3)}\,mo^{-1-\alpha_{l_{gs}}}\,mm^{-\alpha_P}\,yr^{-\alpha_a}}$). As discussed below, g_1 and g_2 are governed by several prominent functional and physiological traits[13,16] and may thus vary with stand characteristics such as soil fertility, leaf type and biome. Equations (1) and (2) can be linearized, respectively, as

$$\ln(\mathrm{NPP}) = \beta_{0,1} + \alpha_p \ln(P) + \alpha_{l_{gs}} \ln(l_{gs}) + \alpha_a \ln(a) - \frac{E}{kT} + \alpha \ln(M_{\mathrm{tot}}) \quad (3)$$

and

$$\ln\left(\frac{\mathrm{NPP}}{l_{gs}}\right) = \beta_{0,2} + \alpha_P \ln(P) + \alpha_a \ln(a) - \frac{E}{kT} + \alpha \ln(M_{\mathrm{tot}}) \quad (4)$$

[1]Department of Ecology and Evolutionary Biology, University of Arizona, Tucson, Arizona 85721, USA. [2]Key Laboratory of Humid Subtropical Eco-geographical Process, Fujian Normal University, Ministry of Education, Fuzhou, Fujian Province 350007, China. [3]Department of Biology, Kenyon College, Gambier, Ohio 43022, USA. [4]The Santa Fe Institute, USA, 1399 Hyde Park Road, Santa Fe, New Mexico 87501, USA. [5]The iPlant Collaborative, Thomas W. Keating Bioresearch Building, 1657 East Helen Street, Tucson, Arizona 85721, USA. [6]Aspen Center for Environmental Studies, 100 Puppy Smith Street, Aspen, Colorado 81611, USA.

where the intercepts are $\beta_{0,1} = \ln(g_1) + \ln(c_n/A) + \ln\left(\left[5c_m^{8/3}/3c_n\right]^{\alpha}\right)$ and $\beta_{0,2} = \ln(g_2) + \ln(c_n/A) + \ln\left(\left[5c_m^{8/3}/3c_n\right]^{\alpha}\right)$.

Evaluating hypothesized drivers of NPP

Here we use equations (3) and (4) to evaluate several long-standing hypotheses for direct and indirect climate effects on global variation in NPP and NPP/l_{gs}. Specifically, we conducted four separate analyses of globally distributed data on woody plant production. Our data set spans broad ranges of temperature and precipitation (Fig. 1a).

First, in agreement with previous reports[2–5], NPP is a significant correlate of mean annual temperature and mean annual precipitation (Fig. 1b, c and Extended Data Table 1). Furthermore, NPP and average annual temperature $<1/kT>_a$ followed an Arrhenius relationship (Fig. 2a and Extended Data Table 1) with an estimated activation energy ($E = 0.296$; 95% confidence interval (CI) = 0.268 to 0.324) that was not different from the hypothesized[15] 0.32 eV. Additionally, NPP was significantly influenced by stand biomass and decreased with plant age (Fig. 1d and Extended Data Table 2).

Second, we examined NPP/l_{gs} (Fig. 2) to assess how climate and ecosystem variables influenced more instantaneous production rates. In contrast to results for NPP, average growing season temperature $<1/kT>_{gs}$, mean annual precipitation, and mean growing season precipitation explained little to no variation in global NPP/l_{gs} (Fig. 2b–d and Extended Data Table 1). The relationship between NPP/l_{gs} and average growing season temperature (Fig. 2b) provided an estimate of $E = -0.067$ eV (95% CI = −0.131 to 0.003) that was significantly lower than and opposite in direction to the hypothesized 0.32 eV (ref. 15). This suggests that local adaptation may dampen the ambient temperature response between communities and that the correlation between NPP and mean annual temperature (Fig. 1b) is spurious. For example, mean annual temperature was strongly correlated with growing season length (Extended Data Fig. 2).

Third, to assess hypothesized drivers of NPP while simultaneously controlling for the influence of all other model covariates, we fitted the complete model (equations (1) and (3)) to the data using multiple regression (Table 1 and Extended Data Fig. 3). A large proportion of variation in NPP (full model adjusted $R^2 = 0.769$) was explained by just two variables: stand biomass and plant age. Importantly, in contrast to pairwise correlations (Fig. 1b, c), this multivariate approach revealed that average growing season temperature (partial $r^2 = 0.073$) and mean growing season precipitation (partial $r^2 = 0.011$) explained little of the variation in NPP, and growing season length explained almost none (partial $r^2 = 0.004$). The mass-scaling exponent was estimated as $\alpha = 0.763$ (95% CI = 0.735 to 0.792), significantly greater than the metabolic scaling theory prediction of 3/5 = 0.60. Furthermore, the scaling exponent for growing season length ($\alpha_{l_{gs}} = 0.058$; 95% CI = −0.007 to 0.109) was significantly lower than the value of 1 required for direct proportionality[7,8]. The estimated activation energy $E = 0.195$ eV (95% CI = 0.156 to 0.234) did not include the hypothesized 0.32 eV. These general conclusions did not change when using mean annual temperature and/or mean annual precipitation, or root, aboveground woody, and foliage components of NPP (Extended Data Table 3).

Comparing the fit of the complete model (equations (1) and (3)) with a simpler model containing only plant age and stand biomass ($NPP = ca^{\alpha_a} M_{tot}^{\alpha}$) yielded similar coefficients of determination but a higher Akaike information criterion (AIC) value for the complete model (AIC = 140.115,

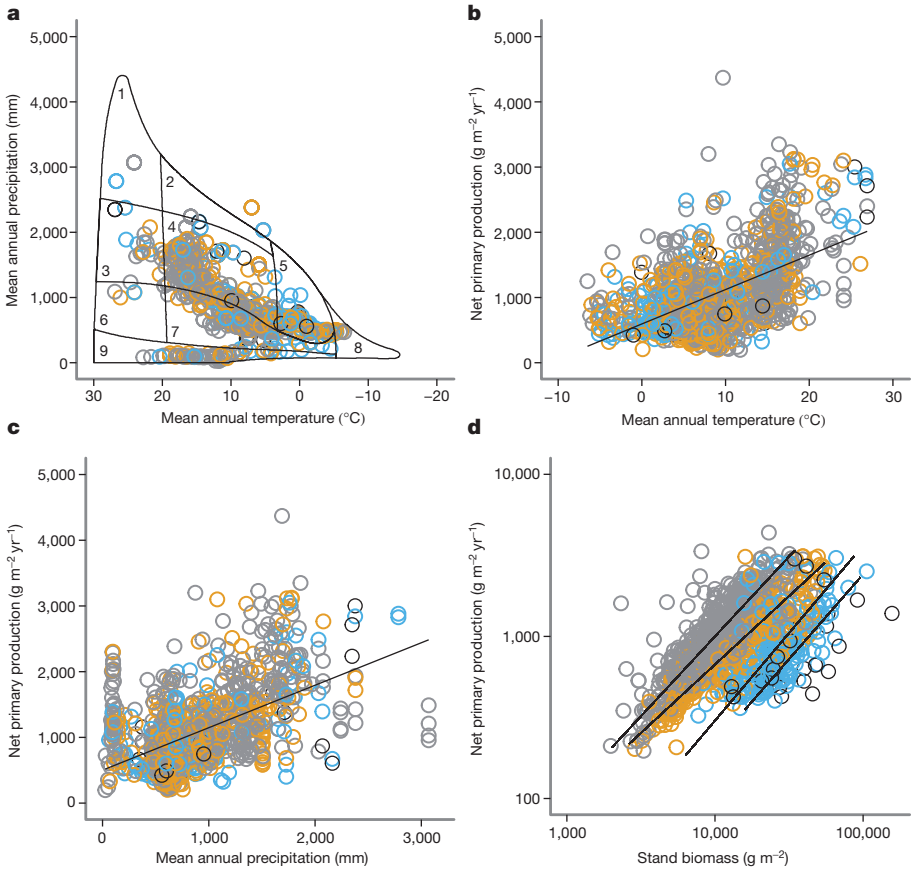

Figure 1 | Global variation in annual net primary production for 1,247 woody plant communities grouped by age class. **a**, Precipitation–temperature space occupied by the plant communities. Biome definitions from ref. 39. 1, tropical rainforest; 2, temperate rainforest; 3, tropical seasonal forest; 4, temperate forest; 5, taiga; 6, savannah; 7, woodland/shrubland; 8, tundra; 9, desert. **b**, Relationship between NPP and mean annual temperature. **c**, Relationship between NPP and mean annual precipitation. **d**, Relationship between NPP and stand biomass. Grey, 0–50 years; orange, 51–100 years; blue, 101–200 years; black, ≥201 years.

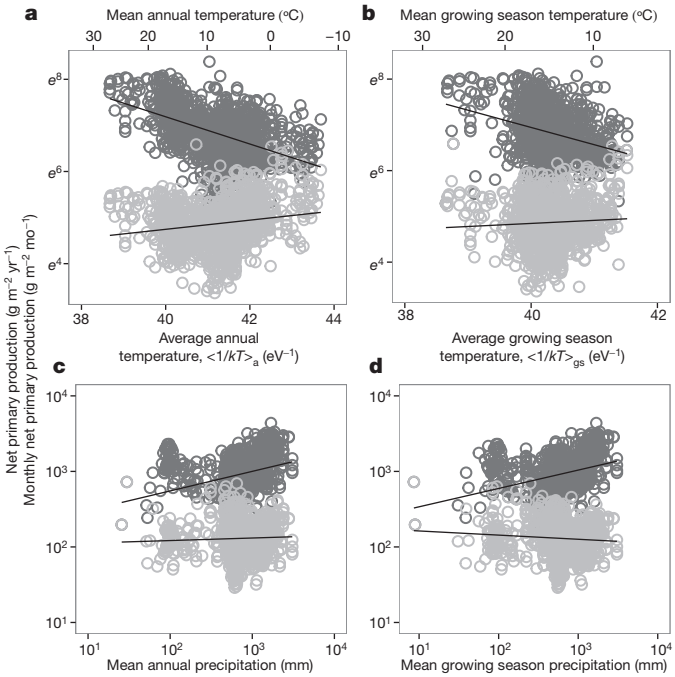

Figure 2 | Net primary production of woody plant communities across global climate gradients. **a**, Annual temperature. **b**, Growing season temperature. **c**, Annual precipitation. **d**, Growing season precipitation. Dark grey, annual net primary production (NPP); light grey, monthly net primary production (NPP/l_{gs}); *e*, mathematical constant (~2.718).

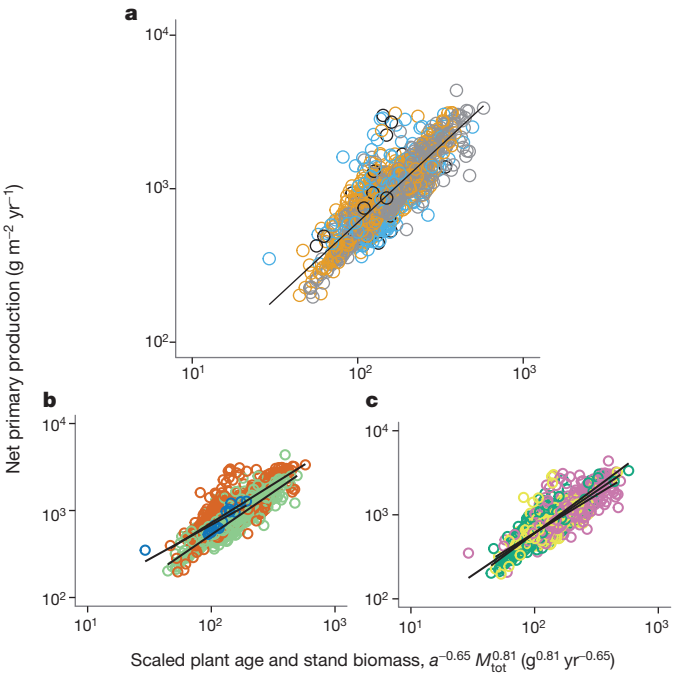

Figure 3 | Global variation in annual net primary production of woody plant communities expressed as a general scaling function of plant age *a* and stand biomass M_{tot}. **a**, 1,247 stands grouped by age class with ordinary least squares (OLS) regression line; **b**, 1,247 stands grouped by leaf functional trait type with standardized major axis (SMA) regression lines; **c**, 1,237 stands grouped by soil fertility class with SMA regression lines. Grey, 0–50 years; light orange, 51–100 years; light blue, 101–200 years; black, ≥201 years; dark orange, broadleaf; light green, needle-leaf; dark blue, mixed-leaf; pink, low soil fertility; yellow, medium soil fertility; dark green, high soil fertility.

$R^2 = 0.769$) than for the simpler model (AIC = −1768.585, $R^2 = 0.735$; Fig. 3a and Extended Data Fig. 4), indicating that age and biomass together explained most of the variation in NPP (Fig. 3a). Soil and leaf trait differences did not influence scaling relationships, but did influence normalization constants (Fig. 3b, c and Supplementary Information). Biome differences affected scaling relationships in some cases and normalization constants in others (Extended Data Fig. 4 and Supplementary Information).

Fourth, because metabolic scaling theory predictions are based on instantaneous rates, a more precise evaluation should consider instantaneous NPP with climate variables most relevant to growth physiology. Therefore, we used multiple regression to assess metabolic scaling theory for rates of NPP/l_{gs} (equations (2) and (4)) using average growing season temperature and mean growing season precipitation (Table 1 and Fig. 4). With these data, all covariates were significant (Table 1). The explanatory ability of this model was reduced (adjusted $r^2 = 0.440$), probably due to error in growing season length estimates. Similar to NPP, stand biomass and plant age were the best predictors of variation in NPP/l_{gs}, with little of the variation explained by mean growing season precipitation (partial $r^2 = 0.095$) and essentially none of the variation explained by average growing season temperature (partial $r^2 = 0.007$). In support of metabolic scaling theory, the mass-scaling exponent was estimated as $\alpha = 0.613$ (95% CI = 0.575 to 0.652), which is indistinguishable from the metabolic scaling theory prediction of 3/5 = 0.60. However, the estimated activation energy $E = -0.079$ (95% CI = −0.130 to 0.028) was significantly lower and opposite in direction to the hypothesized value of $E = 0.32$ eV (ref. 15). These conclusions did not generally change when using root, aboveground woody and foliage components of NPP/l_{gs} (Extended Data Table 3).

Climate has little direct effect on NPP

Our analyses question several long-held and more recent conclusions regarding the influence of climate on global variation in NPP, and reveal that a number of central conclusions established in studies using bivariate regression are probably spurious. For example, mean annual temperature and mean annual precipitation are often cited as primary drivers of NPP (see refs 2–5 and Fig. 1b, c), but after controlling for plant age and stand biomass, temperature and precipitation explained little to none of the variation (Table 1 and Fig. 4a, b). Likewise, hypothesized activation values of 0.32 eV have been supported by bivariate relationships (for example, Fig. 2a and ref. 15), but accounting for other covariates yielded estimates that did not support these predictions[15] (Table 1 and Fig. 4a). These results are intriguing given that the temperature-dependencies of local scale photosynthesis and respiration are well established[6].

Three factors might account for the absence of direct climate effects. First, like most studies in plant ecology and ecosystem metabolism[2,3,7,10,11,16], our analyses considered ambient air temperature. However, air temperatures may not reflect the tissue temperatures that govern plant growth rates, because plant traits (thermophysical properties) can influence energy budgets and decouple plant tissue temperatures from air temperature[17]. This could dampen ambient temperature correlations across climate gradients if, for example, selection adjusts leaf traits to maintain leaf temperatures near photosynthetic optima[18]. As air temperature is one of the most commonly used climate variables in plant and ecosystem ecology, any directional plant–air temperature differences (as recently suggested[18]) will have profound implications for our understanding of plant–climate interactions. Mean annual air temperature may yield especially misleading results, because it can differ substantially from the operative temperatures of organisms, and it also covaries with other key drivers of metabolism and NPP (see, for example, Extended Data Fig. 2) that can act as confounding variables to produce spurious relationships. We suggest that future studies move away from using mean annual air temperature and instead use air and plant body temperatures measured during the growing season and/or key periods of development. Second, biochemical adaptation and/or acclimatization to cold temperatures may increase plant metabolism[7,8,19]. For example, observed shifts in foliar chemistry and metabolic efficiencies have been argued to offset variation in metabolic kinetics across temperature gradients[8,13]. Third, the climate

Table 1 | Multiple regression fits of theory (equations (3) and (4)) to a global compilation of data from 1,247 woody plant communities

Dependent variable	Covariate	Coefficient	Estimate	95% CI	s.e.	t	P value	Partial r^2
NPP ($g\,m^{-2}\,yr^{-1}$)		β_0	9.336	7.758 to 10.914	0.804	11.609	$<2\times10^{-16}$	0.098
	$<1/kT>_{gs}$	E	0.195	0.156 to 0.234	0.020	9.854	$<2\times10^{-16}$	0.073
	a	α_a	−0.568	−0.599 to −0.537	0.016	−35.808	$<2\times10^{-16}$	0.508
	l_{gs}	$\alpha_{l_{gs}}$	0.058	0.007 to 0.109	0.026	2.223	0.026	0.004
	M_{tot}	α	0.763	0.735 to 0.792	0.014	52.863	$<2\times10^{-16}$	0.693
	P_{gs}	α_P	0.043	0.020 to 0.067	0.012	3.664	2.58×10^{-4}	0.011
NPP/l_{gs} ($g\,m^{-2}\,mo^{-1}$)		β_0	−1.652	−3.741 to 0.438	1.065	−1.551	0.121	0.002
	$<1/kT>_{gs}$	E	−0.079	−0.130 to 0.028	0.026	3.016	0.003	0.007
	a	α_a	−0.168	−0.392 to −0.310	0.021	−16.711	$<2\times10^{-16}$	0.184
	M_{tot}	α	0.613	0.575 to 0.652	0.020	30.995	$<2\times10^{-16}$	0.436
	P_{gs}	α_P	−0.168	−0.197 to −0.139	0.015	−11.444	$<2\times10^{-16}$	0.095

$<1/kT>_{gs}$, average growing season temperature; a, age; E, activation energy; l_{gs}, growing season length; M_{tot}, stand biomass; P_{gs}, mean growing season precipitation; α, mass scaling exponent; α_a, age scaling exponent; $\alpha_{l_{gs}}$, growing season length scaling exponent; α_P, precipitation scaling exponent; β_0, intercept.

data used here were interpolated from 29-year climate station means[20] and are not necessarily representative of the years when production data were obtained. Thus, regressing short-term NPP estimates on longer-term climate estimates will add noise to the relationships. Nonetheless, while we are unaware if this error yields a directional bias across climate gradients, future work should assess its importance.

Terrestrial NPP increases asymptotically with precipitation[4,5] because plant growth in terrestrial ecosystems is generally water limited. However, our analyses suggest that this relationship doesn't occur through direct effects of precipitation on plant metabolism per se, but instead via indirect effects of water availability on stand biomass and plant age. Although this is counterintuitive given the importance of water in whole-plant physiology (for example, avoidance of xylem embolism and control of stomatal aperture), it is consistent with a more hydrological view of plant–atmosphere interactions[21]. Specifically, biomass controls the total leaf area that drives transpiration, assimilation and growth. Furthermore, precipitation is not necessarily representative of plant-available water[22], so rather than using precipitation as the primary measure of plant-available water, evapotranspiration[5] should also be included.

Plant age effects on NPP

Even after controlling for stand biomass and climate, global NPP/l_{gs} decreased with age so that (for a given biomass) younger stands had higher rates of production. Although such age-related declines are well documented[23], the drivers of this pattern remain unclear. Numerous mechanisms have been proposed, including: (1) hydraulic limitation of plant height[24]; (2) changes in carbon use efficiency[25], potentially from increasing respiration requirements with size; (3) ontogenetic shifts in biomass allocation, with smaller plants having proportionately more foliage and higher assimilation rates; (4) increasing light limitation with age[26,27]; and (5) decreasing stand density with age[28], which would act through the size-corrected size distribution term c_n. Together, our results reiterate a need in global change studies for a deeper understanding of the causal mechanisms linking age to plant production.

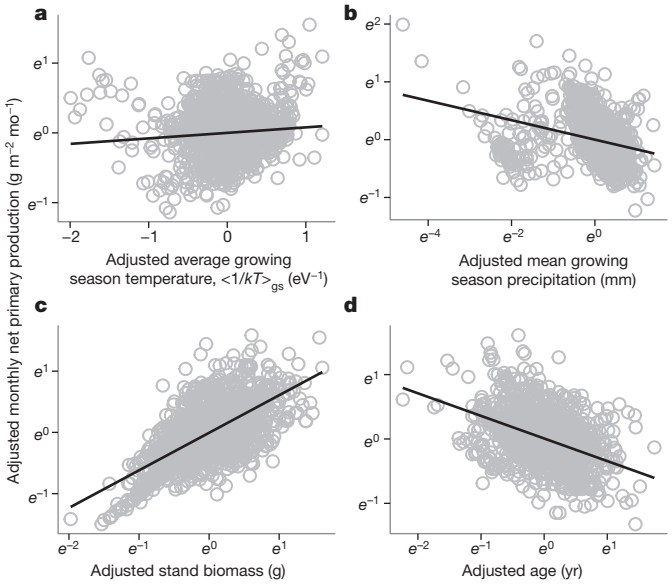

Figure 4 | Partial regression plots illustrating relationships between monthly net primary production (NPP/l_{gs}) and individual covariates from equation (4) for 1,247 woody plant communities. Plots show the correct relationship (slope and variance) between NPP/l_{gs} and each covariate while controlling for the influence of all other model covariates. **a**, Average growing season temperature; **b**, mean growing season precipitation; **c**, stand biomass; **d**, plant age; e, mathematical constant (~2.718).

Climate controls NPP via biomass and age

Whereas temperature and water availability are fundamental drivers of plant physiology and ecosystem metabolism at local scales[19,29,30], at global scales they appear to have little direct kinetic control on NPP. Instead, our findings suggest that climate influences NPP indirectly via plant age and stand biomass (see ref. 11), which is largely driven by maximum plant size[31,32]. For example, plant age is influenced by time since last disturbance, and maximum plant size is constrained by limitations on the water and energy fluxes necessary to support basal metabolism[24,31,32].

Our theoretical framework further extends the predictive ability of metabolic scaling theory and links multiple hypothesized climate drivers to plant and ecosystem metabolism. Furthermore, it uniquely (1) integrates metabolic scaling and physiological approaches to plant ecology and global change studies; (2) underscores the importance of plant size, allometry and age as primary drivers of variation in ecosystem metabolism; and (3) provides a foundation to assess if adaptive differences in plant form and function can compensate for broad-scale climate gradients. Although our results support the mechanistic basis of metabolic scaling theory for the origin of the ecosystem mass-scaling exponent α (see ref. 11) and the influence of plant traits on variation in the normalization constants g_1 and g_2, they also highlight a need for integrative theory that explains the age-dependence of terrestrial NPP (estimated here as $\alpha_a = -0.65$). Additionally, future work is needed on the geographical scale at which the activation energy for plant metabolism becomes decoupled from temperature.

We have shown that global variation in terrestrial NPP is consistent with the hypothesis that the diversity of plant form and function originated via selection to maximize plant growth across climate gradients[7,8] (Fig. 4). This has resulted in convergence to a common scaling relationship between NPP, plant age and total stand biomass (Fig. 3). Interestingly, recent analyses indicate that both mean annual temperature and mean annual precipitation are also poor predictors of total stand biomass[32] (but see ref. 33). Additionally, metabolic scaling theory predicts[11,12] and recent empirical data show[32,34] that the best predictor of total autotrophic ecosystem biomass appears to be the size of the largest individual. Consequently, efforts to predict ecosystem function in response to global change should include the mechanisms that govern maximum plant size[31] and general ecosystem scaling relationships (Fig. 3).

METHODS SUMMARY

We assessed variation in NPP and NPP/l_{gs} across broad climate gradients using a global compilation of biomass and production data for 1,247 woody plant communities[8,35–38] (and Malhi, Y. *et al*, submitted) and climate data from a high-resolution gridded data set[20] (see Methods). NPP was computed as the sum of annual production of root, stem, branch, reproductive (when available) and foliage components. To calculate NPP/l_{gs}, growing season length was calculated as the number of months with a mean minimum temperature greater than 0.6 °C and a moisture index MI > 0.048 (ref. 8). Temperature and precipitation were calculated as both annual and growing season averages, and temperature was also expressed as the Boltzmann factor exponent $1/kT$. Relationships between production and climate variables were first assessed using OLS linear regression. Next, equations (3) and (4) were fit to compiled data to evaluate relationships between NPP or NPP/l_{gs} and hypothesized drivers. Finally, the fit of the complete model (equations (1) and (3)) was competed with that of a simpler model ($\mathrm{NPP} = ca^{\alpha_a} M_{\mathrm{tot}}^{\alpha}$) obtained via multiple regression with age and biomass as covariates.

Online Content Methods, along with any additional Extended Data display items and Source Data, are available in the online version of the paper; references unique to these sections appear only in the online paper.

Received 23 December 2013; accepted 12 May 2014.
Published online 20 July; corrected online 6 August 2014 (see full-text HTML version for details).

1. Schimel, D. S. *et al.* Recent patterns and mechanisms of carbon exchange by terrestrial ecosystems. *Nature* **414,** 169–172 (2001).
2. Lieth, H. in *Primary Productivity of the Biosphere* (eds Lieth, H. & Whittaker, R. H.) (Springer, 1975).
3. Schuur, E. A. G. Productivity and global climate revisited: The sensitivity of tropical forest growth to precipitation. *Ecology* **84,** 1165–1170 (2003).
4. Huxman, T. E. *et al.* Convergence across biomes to a common rain-use efficiency. *Nature* **429,** 651–654 (2004).
5. Ponce Campos, G. E. *et al.* Ecosystem resilience despite large-scale altered hydroclimatic conditions. *Nature* **494,** 349–352 (2013).
6. Berry, J. & Bjorkman, O. Photosynthetic response and adaptation to temperature in higher plants. *Annu. Rev. Plant Physiol.* **31,** 491–543 (1980).
7. Enquist, B. J., Kerkhoff, A. J., Huxman, T. E. & Economo, E. P. Adaptive differences in plant physiology and ecosystem paradoxes: insights from metabolic scaling theory. *Glob. Change Biol.* **13,** 591–609 (2007).
8. Kerkhoff, A. J., Enquist, B. J., Elser, J. J. & Fagan, W. F. Plant allometry, stoichiometry and the temperature-dependence of primary productivity. *Glob. Ecol. Biogeogr.* **14,** 585–598 (2005).
9. Bonan, G. B. Physiological derivation of the observed relationship between net primary production and mean annual air temperature. *Tellus B Chem. Phys. Meterol.* **45,** 397–408 (1993).
10. Chapin, F. S. Effects of plant traits on ecosystem and regional processes: A conceptual framework for predicting the consequences of global change. *Ann. Bot. (Lond.)* **91,** 455–463 (2003).
11. Enquist, B. J., West, G. B. & Brown, J. H. Extensions and evaluations of a general quantitative theory of forest structure and dynamics. *Proc. Natl Acad. Sci. USA* **106,** 7046–7051 (2009).
12. West, G. B., Enquist, B. J. & Brown, J. H. A general quantitative theory of forest structure and dynamics. *Proc. Natl Acad. Sci. USA* **106,** 7040–7045 (2009).
13. Enquist, B. J. *et al.* A general integrative model for scaling plant growth, carbon flux, and functional trait spectra. *Nature* **449,** 218–222 (2007).
14. Brown, J. H., Gillooly, J. F., Allen, A. P., Savage, V. M. & West, G. B. Toward a metabolic theory of ecology. *Ecology* **85,** 1771–1789 (2004).
15. Allen, A. P., Gillooly, J. F. & Brown, J. H. Linking the global carbon cycle to individual metabolism. *Funct. Ecol.* **19,** 202–213 (2005).
16. Enquist, B. J. & Bentley, L. P. in *Metabolic Ecology: A Scaling Approach* (eds Sibly, R. M., Brown, S. & Kodric-Brown, A.) 164–187 (Wiley, 2012).
17. Gates, D. M. *Biophysical Ecology* (Springer, 1980).
18. Helliker, B. R. & Richter, S. L. Subtropical to boreal convergence of tree-leaf temperatures. *Nature* **454,** 511–514 (2008).
19. Atkin, O. K. & Tjoelker, M. G. Thermal acclimation and the dynamic response of plant respiration to temperature. *Trends Plant Sci.* **8,** 343–351 (2003).
20. New, M., Lister, D., Hulme, M. & Makin, I. A high-resolution data set of surface climate over global land areas. *Clim. Res.* **21,** 1–25 (2002).
21. Monteith, J. L. Climate and the efficiency of crop production in Britain. *Phil. Trans. R. Soc. Lond. B* **281,** 277–294 (1977).
22. Renee Brooks, J., Barnard, H. R., Coulombe, R. & McDonnell, J. J. Ecohydrologic separation of water between trees and streams in a Mediterranean climate. *Nature Geosci.* **3,** 100–104 (2010).
23. Gower, S. T., McMurtrie, R. E. & Murty, D. Aboveground net primary production decline with stand age: potential causes. *Trends Ecol. Evol.* **11,** 378–382 (1996).
24. Ryan, M. G. & Yoder, B. J. Hydraulic limits to tree height and tree growth. *Bioscience* **47,** 235–242 (1997).
25. DeLucia, E. H., Drake, J. E., Thomas, R. B. & Gonzalez-Meler, M. Forest carbon use efficiency: is respiration a constant fraction of gross primary production? *Glob. Change Biol.* **13,** 1157–1167 (2007).
26. Kerkhoff, A. J. & Enquist, B. J. Ecosystem allometry: the scaling of nutrient stocks and primary productivity across plant communities. *Ecol. Lett.* **9,** 419–427 (2006).
27. Muller-Landau, H. C. *et al.* Testing metabolic ecology theory for allometric scaling of tree size, growth, and mortality in tropical forests. *Ecol. Lett.* **9,** 575–588 (2006).
28. Niklas, K. J., Midgley, J. J. & Rand, R. H. Tree size frequency distributions, plant density, age and community disturbance. *Ecol. Lett.* **6,** 405–411 (2003).
29. Yvon-Durocher, G. *et al.* Reconciling the temperature dependence of respiration across timescales and ecosystem types. *Nature* **487,** 472–476 (2012).
30. Wright, I. J. & Westoby, M. Differences in seedling growth behaviour among species: trait correlations across species, and trait shifts along nutrient compared to rainfall gradients. *J. Ecol.* **87,** 85–97 (1999).
31. Kempes, C. P., West, G. B., Crowell, K. & Girvan, M. Predicting maximum tree heights and other traits from allometric scaling and resource limitations. *PLoS ONE* **6,** e20551 (2011).
32. Stegen, J. C. *et al.* Variation in above-ground forest biomass across broad climatic gradients. *Glob. Ecol. Biogeogr.* **20,** 744–754 (2011).
33. Larjavaara, M. & Muller-Landau, H. C. Rethinking the value of high wood density. *Funct. Ecol.* **24,** 701–705 (2010).
34. Stephenson, N. L. *et al.* Rate of tree carbon accumulation increases continuously with tree size. *Nature* **507,** 90–93 (2014).
35. Cannell, M. G. R. *World Forest Biomass and Primary Production Data* (Academic, 1982).
36. Luo, T. X. *Patterns of Biological Production and its Mathematical Models for Main Forest Types of China*. PhD thesis, Chinese Academy of Sciences (1996).
37. Clark, D. S. *et al.* Net primary productivity in tropical forests: An evaluation and synthesis of existing field data. *Ecol. Appl.* **11,** 371–384 (2001).
38. Luyssaert, S. *et al.* CO_2 balance of boreal, temperate, and tropical forests derived from a global database. *Glob. Change Biol.* **13,** 2509–2537 (2007).
39. Whittaker, R. H. *Communities and Ecosystems* (Macmillan, 1970).

Supplementary Information is available in the online version of the paper.

Acknowledgements S.T.M. and B.J.E. were supported by an NSF MacroSystems award (1065861) and a fellowship from the Aspen Center for Environmental Studies. D.C. was supported by the National Natural Science Foundation of China (31170374 and 31370589) and Fujian Natural Science Funds for Distinguished Young Scholar (2013J06009). A.J.K. was supported by a sabbatical supplement from Kenyon College, and by a National Science Foundation ROA supplement (1065861) to the NSF MacroSystems award (1065861) to B.J.E.

Author Contributions S.T.M., D.C., A.J.K. and B.J.E. compiled data, developed theory, performed analyses and wrote the paper.

Author Information Reprints and permissions information is available at www.nature.com/reprints. The authors declare no competing financial interests. Readers are welcome to comment on the online version of the paper. Correspondence and requests for materials should be addressed to B.J.E. (benquist@email.arizona.edu) or D.C. (chengdl@fjnu.edu.cn).

METHODS

Woody plant biomass and production data. Woody plant biomass and production data comprising both above- and belowground components were compiled from multiple data sources (see Source Data file associated with the figures). First, the Cannell[35] data set that summarizes data from over 1,200 stands in 46 countries. Second, the Luo[36] data set comprising data from over 5,000 forest stands across broad climate gradients in China. Third, we examined the primary references in recent publications[8,37,38] (and Malhi, Y. *et al*, submitted) and online data compilations (https://daac.ornl.gov/NPP/guides/NPP_EMDI.html) and included data from 41 additional sites. A complete list of data source references is provided in the Source Data file associated with the figures. Together, the compiled sites span most of the climate space in a plot of mean annual precipitation versus mean annual temperature (Fig. 1a). Data were compiled for woody conifers, monocots and dicots growing in single- and mixed-species stands, and included latitude, longitude, plant age, leaf type of dominant species, biome, above- and belowground dry biomass, and above- and belowground net production. For each stand, NPP (g m^{-2} yr^{-1}) was calculated by summing estimated annual biomass production of roots, stems, branches, reproductive structures (when available) and foliage. When biomass and production data were reported in grams of carbon, data were converted to grams of biomass assuming biomass is 50% carbon. Belowground biomass and production data were not available for four sites (Index 1218-1221 in Source Data associated with Fig. 1), so these were estimated by multiplying the aboveground values by 0.21 based on published data[40]. Age data were not available for thirteen old growth Amazonian forests (described in Malhi, Y. *et al*, submitted, and Source Data associated with the figures), so ages were estimated by multiplying the reported woody biomass residence times by a factor of 3.77 based on published data for canopy and emergent trees from two old growth Amazonian forests[41]; note that for these old growth forests, the age of the dominant size classes (that is, canopy and emergent trees) is most relevant, because these individuals constitute most of the stand biomass. For the Luyssaert data set[38], we selected sites where biomass and production were both measured within a period of one year or less. Analyses considered only natural (non-plantation) stands for which published above- and belowground biomass and production data were available, giving a total of 1,247 stands from Africa, Asia, Europe, North America and South America.

Climate data. Climate data for each stand were obtained from a global 10-min resolution gridded climatology[20] (see Source Data file associated with the figures). Temperature and precipitation were calculated as both annual and growing season values. Mean annual temperature (°C) was calculated as the 12-month average of mean monthly air temperatures, while growing season temperature (°C) was calculated as the average across growing season months only. Temperature was also expressed as the Boltzmann factor exponent $1/kT$, where k is the Boltzmann constant (8.617×10^{-5} eV K^{-1}) and T is temperature (K), and calculated as the annual and growing season averages $<1/kT>_a$ and $<1/kT>_{gs}$, respectively. Mean annual precipitation P_a (mm) was taken as the 12-month sum of mean monthly values, and mean growing season precipitation P_{gs} (mm) was calculated as the sum across growing season months.

Growing season months were defined as months with a mean minimum temperature greater than 0.6 °C and a moisture index MI > 0.048. These thresholds were calibrated from our data, as they are the maximum values that result in a growing season length of at least one month for all sites. The calibrated thresholds agree with empirical air temperature[42] and precipitation[8] limits for woody plant growth. Minimum temperature data were calculated from monthly temperature means and ranges. The moisture index is a relative measure of availability and demand for water and was taken as MI = PPT/PET, where PPT is monthly mean precipitation (mm) and PET is monthly potential evapotranspiration (mm mo^{-1}; calculated using the Thornthwaite method, assuming 30 days in each month[43]). The MI threshold should provide a growing season length of at least one month for all sites where plants grow. However, as the threshold is increased, it results in sites with low MI being assigned a zero month growing season. Our analyses used MI = 0.048, as this is the maximum value that gives a growing season length of at least one month for all sites, and thus the MI threshold is calibrated using the data set. This threshold agrees with an independently calibrated threshold of MI = 0.05 used in Kerkhoff *et al.* (ref. 8). Since these growing season estimates are calculated from long-term climate averages and not site-specific phenology data, they are subject to error, but the simplicity and consistency of this approach is appropriate given the large number of sites considered in the analyses.

Soil data. Soil data for 1,237 stands were obtained from a global 30 arcsec raster soil database[44] (see Source Data file associated with the figures). Stands were classified into low (lower tertile), medium (middle tertile) and high (upper tertile) soil fertility classes based on the mean of topsoil and subsoil total exchangeable bases (TEB). TEB is the sum of the exchangeable base cations Ca^{2+}, Mg^{2+}, K^+ and Na^+, and is an index of soil fertility as it strongly correlates with a large number of soil properties that influence fertility and plant-available nutrients[45].

Statistical analyses. Relationships between NPP and mean annual temperature or mean annual precipitation were described using ordinary least squares (OLS) linear regression in the statistical software R (ref. 46). To characterize the biomass-scaling of NPP, forest stands were first divided into four age classes (0–50 years, 51–100 years, 101–200 years, and ≥201 years) to reduce bias in estimates of scaling exponents α resulting from age-related declines in NPP. Mass-scaling terms M_{tot}^{α} were then obtained by model II (SMA) regression of NPP and biomass data using sma() from the R package smatr[47]. SMA slopes were significantly heterogeneous among age classes ($P = 2.158 \times 10^{-5}$), so unique slopes were calculated for each age class. Relationships between production (NPP or NPP/l_{gs}) and climate (average annual temperature $<1/kT>_a$, average growing season temperature $<1/kT>_{gs}$, mean annual precipitation, and mean growing season precipitation) were identified using OLS linear regression.

The complete models (equations (1) to (4)) were then fit to compiled data using multiple regression in R. Since NPP/l_{gs} and $<1/kT>_{gs}$ are non-independent, their shared term l_{gs} may give rise to spurious correlations[48], but this was not observed for our data (Table 1). To evaluate potential collinearity problems that may arise from linear relationships between model covariates[49], we calculated variance-inflation factors (VIFs) for each covariate in each model using vif() from the package car in R. VIFs for all covariates were lower than 2, far less than the threshold of 10 above which collinearity may adversely affect regression results[49]. Functional forms for precipitation- and age-dependence of NPP in equation (1) were assessed using partial residual plots (Supplementary Information and Extended Data Fig. 1) obtained using crPlots() from the R package car. Partial regression statistics were obtained using lm.sumSquares() from the R package lmSupport, and partial regression plots were prepared using avPlots() from the car package. Partial regression plots show the correct strength of the relationship between the dependent variable and each independent variable while controlling for the influence of all other independent variables included in the model; plotted variables are residuals, so the slope and variance equal the partial estimates from the multiple regression model.

Finally, the fit of the complete model (equations (1) and (3)) was compared with that of a simpler model ($NPP = ca^{\alpha_a} M_{tot}^{\alpha}$) obtained via multiple regression with stand age and biomass as covariates (but not temperature or precipitation, which are implicit in the normalization constant c). For this simpler model, differences in slope and elevation among leaf types (broadleaf, needle-leaf, and mixed-leaf), fertility classes (low, medium, high) and biomes were assessed using likelihood ratio and Wald statistics, respectively, from SMA[47] fits of NPP on $a^{\alpha_a} M_{tot}^{\alpha}$ (where α_a and α were first obtained as described above). Sites were assigned to biomes using mean annual temperature and precipitation data and standard biome definitions[39], although more detailed descriptions from original data sources are provided in the Source Data file associated with the figures. For biomes, SMA regressions were only applied to groups for which the range of $a^{-0.65} M_{tot}^{0.81}$ varied by a factor of five or more (as smaller ranges resulted in weakly positive or negative slopes), thus excluding slope and elevation tests for savannah, temperate rainforest, tropical rainforest, tropical seasonal forest, and tundra biomes.

40. Cairns, M. A., Brown, S., Helmer, E. H. & Baumgardner, G. A. Root biomass allocation in the world's upland forests. *Oecologia* **111,** 1–11 (1997).
41. Vieira, S. *et al.* Slow growth rates of Amazonian trees: Consequences for carbon cycling. *Proc. Natl Acad. Sci. USA* **102,** 18502–18507 (2005).
42. Häsler, R., Streule, A. & Turner, H. Shoot and root growth of young Larix decidua in contrasting microenvironments near the Alpine timberline. *Phyton* **39,** 47–52 (1999).
43. Fredlund, D. G., Rahardjo, H. & Fredlund, M. D. *Unsaturated Soil Mechanics in Engineering Practice* (Wiley, 2012).
44. FAO/IIASA/ISRIC/ISSCAS/JRC. *Harmonized World Soil Database* (version 1.2) (FAO and IIASA, 2012).
45. Huston, M. A. Precipitation, soils, NPP, and biodiversity: resurrection of Albrecht's curve. *Ecol. Monogr.* **82,** 277–296 (2012).
46. R Development Core Team. R: A Language and Environment for Statistical Computing (R Foundation for Statistical Computing, 2011).
47. Warton, D. I., Duursma, R. A., Falster, D. S. & Taskinen, S. smatr 3– an R package for estimation and inference about allometric lines. *Methods Ecol. Evol.* **3,** 257–259 (2012).
48. Brett, M. T. When is a correlation between non-independent variables "spurious"? *Oikos* **105,** 647–656 (2004).
49. Ryan, T. P. *Modern Regression Methods* (Wiley, 1997).

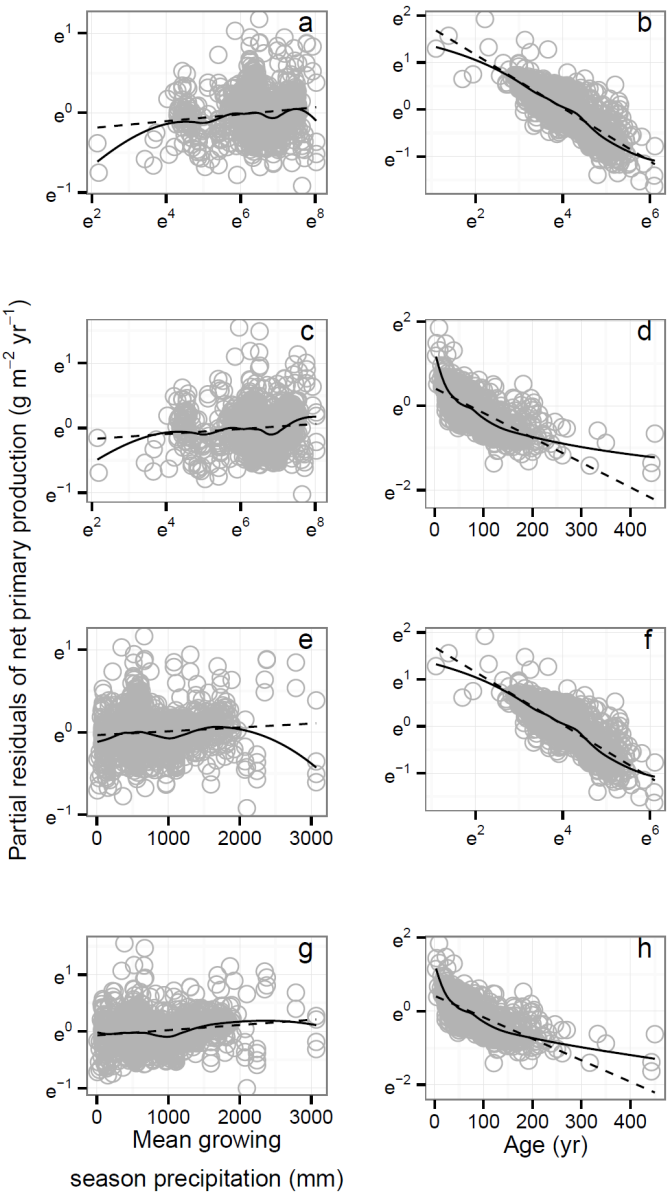

Extended Data Figure 1 | Partial residual plots showing linearization of NPP relationships by power and exponential transforms of precipitation and plant age. Relationships were best linearized by power transforms of both precipitation and age, so power laws were used to characterize precipitation- and age-dependence of NPP in Supplementary Information Equation (S6). Multiple regression models used average growing season temperatures $<1/kT>_{gs}$ and mean growing season precipitation P_{gs}, but similar results were observed using mean annual estimates. Dashed line, OLS linear regression line; solid line, Loess smooth. **a**, **b**, Power transform for precipitation and age; **c**, **d**, power transform for precipitation and exponential transform for age; **e**, **f**, exponential transform for precipitation and power transform for age; **g**, **h**, exponential transform for precipitation and age.

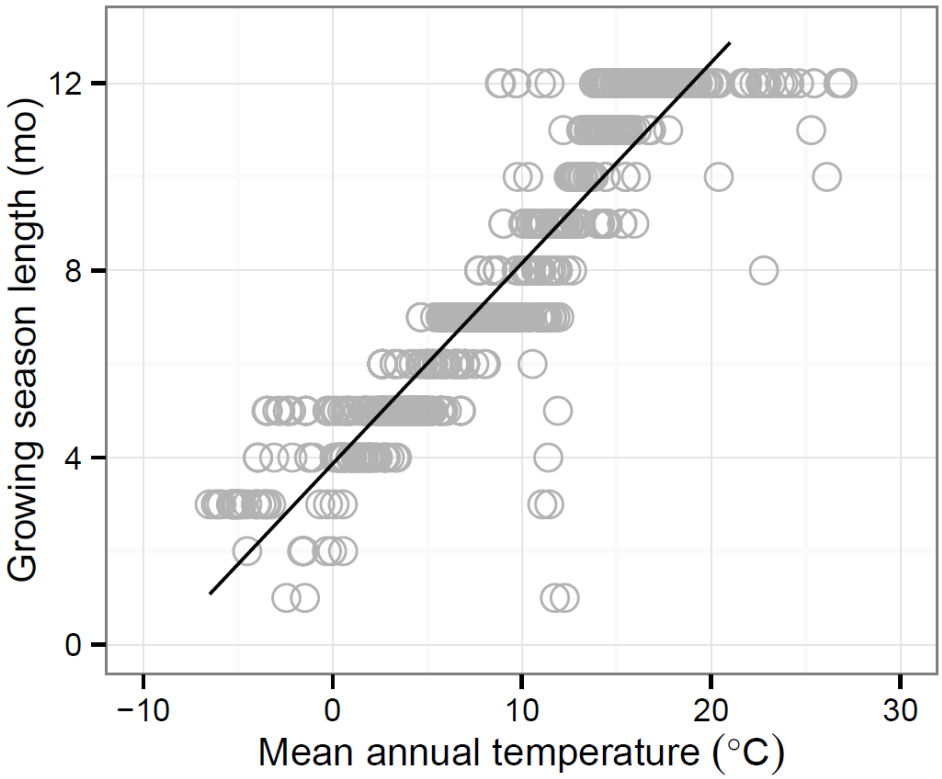

Extended Data Figure 2 | Relationship between mean annual temperature and growing season length ($r^2 = 0.853$, $P < 2.2 \times 10^{-16}$).

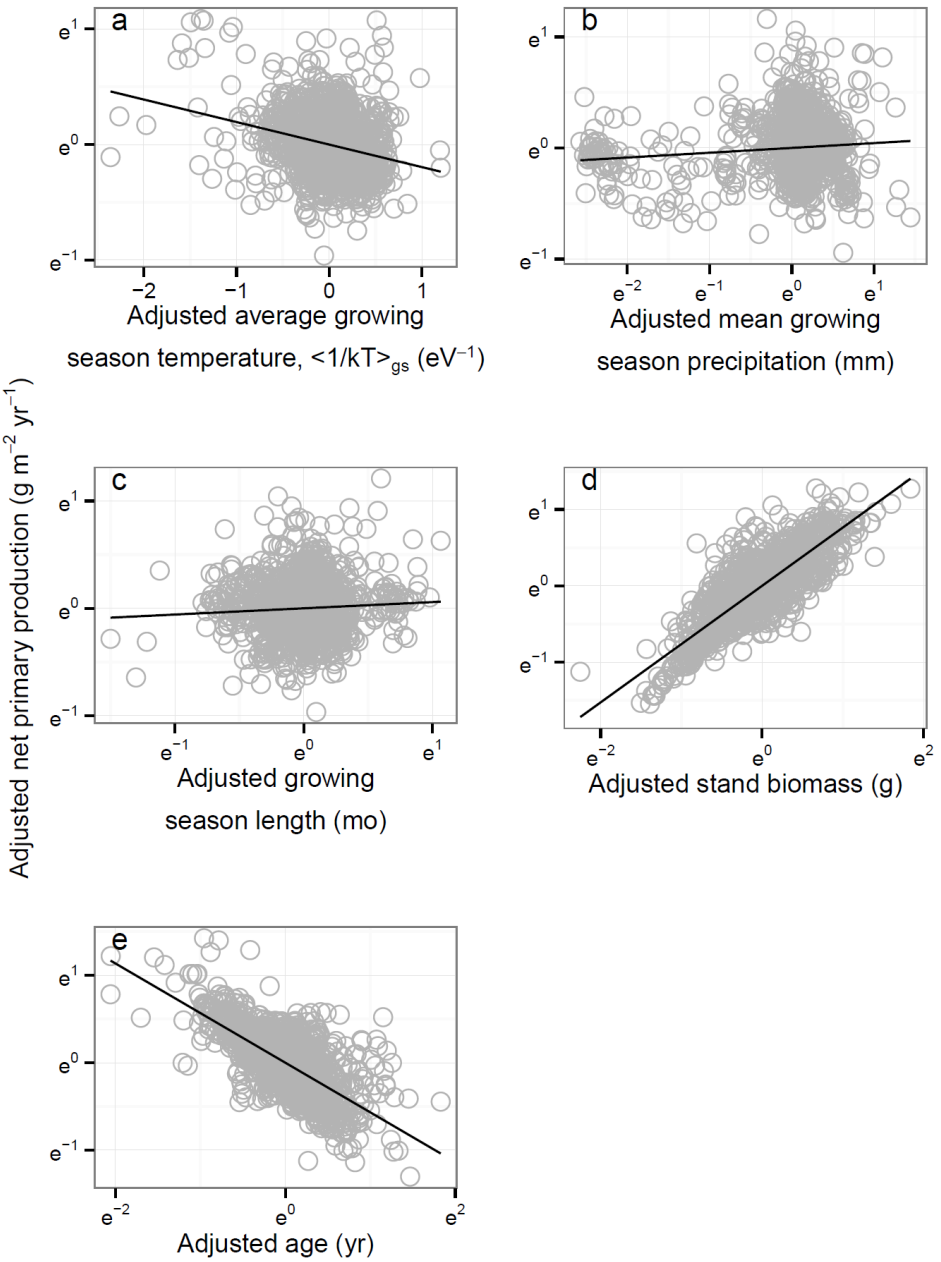

Extended Data Figure 3 | Partial regression plots showing relationships between annual net primary production (NPP) and each covariate. Both variables in each plot are residuals. Plots show the correct relationship (slope and variance) between NPP and each covariate while controlling for the influence of all other model covariates. All relationships were significant at $\alpha = 0.001$, except for growing season length ($P = 0.026$). However, total stand biomass and plant age explained most of the variation in NPP, while temperature, growing season length, and mean annual precipitation each explained less than 10% of the variation (Table 1). **a**, Relationship between NPP and average growing season temperature $<1/kT>_{gs}$. **b**, Relationship between NPP and mean growing season precipitation P_{gs}. **c**, Relationship between NPP and growing season length l_{gs}. **d**, Relationship between NPP and total stand biomass M_{tot}. **e**, Relationship between NPP and plant age a.

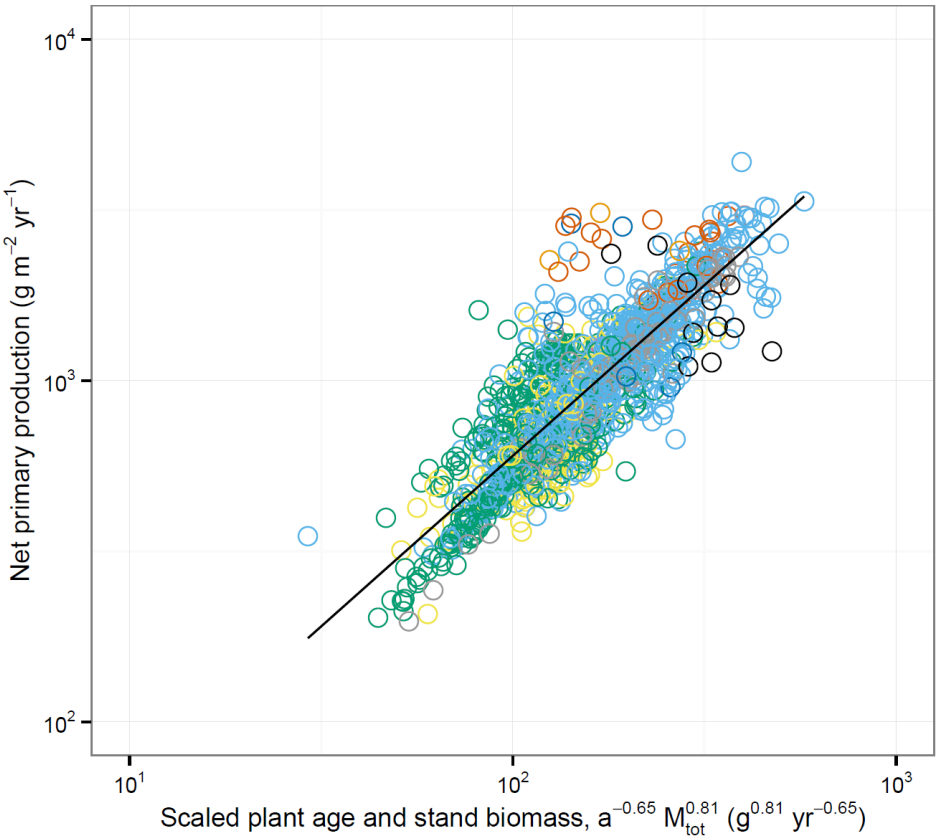

Extended Data Figure 4 | Global variation in annual net primary production (NPP) for 1,247 forest stands expressed as a general scaling function of age *a* and total stand biomass M_{tot}. Stands grouped according to standard biome definitions[39]. Grey, desert; light orange, savannah; light blue, temperate forest; black, temperate rainforest; yellow, taiga; dark blue, tropical rainforest; dark orange, tropical seasonal forest; pink, tundra; green, woodland/shrubland.

Extended Data Table 1 | Bivariate regression fits of net primary production on temperature and precipitation data for 1,247 woody plant communities

Dependent variable	Independent variable	*P* value	r^2
NPP	T_a	$< 2.2 \times 10^{-16}$	0.305
	P_a	$< 2.2 \times 10^{-16}$	0.279
	$<1/kT>_a$	$< 2.2 \times 10^{-16}$	0.256
NPP/l_{gs}	$<1/kT>_{gs}$	0.040	0.003
	P_a	0.121	0.002
	P_{gs}	0.025	0.004

Relationships are plotted in Figs 1b, c and 2. $<1/kT>_a$, average annual temperature; $<1/kT>_{gs}$, average growing season temperature; NPP, annual net primary production; NPP/l_{gs}, monthly net primary production; P_a, mean annual precipitation; P_{gs}, mean growing season precipitation; T_a, mean annual temperature.

Extended Data Table 2 | Standardized major axis (SMA) regression fits of annual net primary production (NPP) on stand biomass for 1,247 woody plant communities

Age class	Mass-scaling exponent α	*P* value	r^2
0-50	0.985	$< 2.2 \times 10^{-16}$	0.717
51-100	0.845	$< 2.2 \times 10^{-16}$	0.636
101-200	1.081	$< 2.2 \times 10^{-16}$	0.361
≥ 200	1.047	0.006	0.262

Relationships are plotted in Fig. 1d.

Extended Data Table 3 | Multiple regression fits of metabolic scaling theory for terrestrial net primary production (equations (3) and (4)) to a global compilation of data for root (subscript R; 1,236 stands), aboveground woody (subscript AGW; 1,233 stands) and foliage (subscript F; 1,234 stands) components of net primary production

Dependent variable	Covariate	Coefficient	Estimate	95% CI	s.e.	*t*	*P* value	Partial r^2
NPP_R (g m^{-2} yr^{-1})		β_0	10.268	7.122 to 13.414	1.604	6.403	2.17×10^{-10}	0.032
	$\langle 1/kT \rangle_{gs}$	E	0.277	0.199 to 0.355	0.040	7.009	3.93×10^{-12}	0.038
	a	α_a	-0.826	-0.889 to -0.764	0.032	-26.093	$< 2 \times 10^{-16}$	0.356
	l_{gs}	$\alpha_{l_{gs}}$	-0.322	-0.423 to -0.221	0.052	-6.243	5.90×10^{-10}	0.031
	M_{tot}	α	0.879	0.823 to 0.935	0.029	30.745	$< 2 \times 10^{-16}$	0.435
	P_{gs}	α_P	0. 187	0.141 to 0.233	0.023	8.012	2.61×10^{-15}	0.050
NPP_{AGW} (g m^{-2} yr^{-1})		β_0	3.604	1.655 to 5.552	0.993	3.627	2.98×10^{-4}	0.011
	$\langle 1/kT \rangle_{gs}$	E	0.090	0.042 to 0.138	0.025	3.679	2.44×10^{-4}	0.011
	a	α_a	-0.792	-0.830 to -0.754	0.020	-40.375	$< 2 \times 10^{-16}$	0.571
	l_{gs}	$\alpha_{l_{gs}}$	0.084	0.022 to 0.147	0.032	2.636	0.009	0.006
	M_{tot}	α	0.919	0.884 – 0.953	0.018	51.872	$< 2 \times 10^{-16}$	0.687
	P_{gs}	α_P	0.056	0.028 – 0.085	0.015	3.887	1.07×10^{-4}	0.012
NPP_F (g m^{-2} yr^{-1})		β_0	9.553	6.209 – 12.897	1.704	5.605	2.57×10^{-8}	0.025
	$\langle 1/kT \rangle_{gs}$	E	0.201	0.119 to 0.283	0.042	4.784	1.92×10^{-6}	0.018
	a	α_a	-0.220	-0.286 to -0.154	0.034	-6.542	8.89×10^{-11}	0.034
	l_{gs}	$\alpha_{l_{gs}}$	0.197	0.089 to 0.304	0.055	3.593	3.40×10^{-4}	0.010
	M_{tot}	α	0.533	0.474 to 0.593	0.030	17.557	$< 2 \times 10^{-16}$	0.201
	P_{gs}	α_P	-0.029	-0.078 to 0.020	0.025	-1.177	0.239	0.001
NPP_R / l_{gs} (g m^{-2} mo^{-1})		β_0	-5.362	-8.965 to -1.759	1.837	-2.919	0.036	0.007
	$\langle 1/kT \rangle_{gs}$	E	-0.113	-0.201 to 0.024	0.045	-2.493	0.013	0.005
	a	α_a	-0.521	-0.593 to -0.450	0.036	-14.350	$< 2 \times 10^{-16}$	0.143
	M_{tot}	α	0.669	0.602 to 0.735	0.034	19.714	$< 2 \times 10^{-16}$	0.240
	P_{gs}	α_P	-0.109	-0.159 to -0.060	0.025	-4.352	1.46×10^{-5}	0.015
NPP_{AGW} / l_{gs} (g m^{-2} mo^{-1})		β_0	-7.228	-9.558 to -4.898	1.188	-6.086	1.55×10^{-9}	0.029
	$\langle 1/kT \rangle_{gs}$	E	-0.180	-0.237 to -0.123	0.029	-6.160	9.81×10^{-10}	0.030
	a	α_a	-0.580	-0.626 to -0.534	0.024	-24.703	$< 2 \times 10^{-16}$	0.332
	M_{tot}	α	0.773	0.729 to 0.816	0.022	35.237	$< 2 \times 10^{-16}$	0.503
	P_{gs}	α_P	-0.149	-0.181 to -0.117	0.016	-9.195	$< 2 \times 10^{-16}$	0.064
NPP_F / l_{gs} (g m^{-2} mo^{-1})		β_0	0.061	-3.292 to 3.414	1.709	0.036	0.972	0.000
	$\langle 1/kT \rangle_{gs}$	E	-0.036	-0.118 to 0.047	0.042	0.848	0.397	0.001
	a	α_a	-0.035	-0.101 to 0.032	0.034	-1.025	0.306	0.001
	M_{tot}	α	0.405	0.344 to 0.467	0.032	12.855	$< 2 \times 10^{-16}$	0.119
	P_{gs}	α_P	-0.210	-0.255 to -0.164	0.023	-8.970	$< 2 \times 10^{-16}$	0.062

$\langle 1/kT \rangle_{gs}$, average growing season temperature; a, age; E, activation energy; l_{gs}, growing season length; M_{tot}, stand biomass; P_{gs}, mean growing season precipitation; α, mass scaling exponent; α_a, age scaling exponent; $\alpha_{l_{gs}}$, growing season length scaling exponent; α_P, precipitation scaling exponent; β_0, intercept.